

## SUPPORTING INFORMATION

### Slippery Liquid-Immobilized Coating Films Using In Situ Oxidation–Reduction Reactions of Metal Ions in Polyelectrolyte Films

*Yosuke Tsuge, Takeo Moriya, Yukari Moriyama, Yuki Tokura and Seimei Shiratori\**

Department of Integrated Design Engineering, Faculty of Science and Technology, Keio  
University, 3-14-1 Hiyoshi, Kohoku-ku, Yokohama, Kanagawa 223-8522 Japan

Corresponding Author: shiratori@appi.keio.ac.jp

#### **Table of Contents**

|       |  |
|-------|--|
| S-1   | Cover page   |
| S-2   | Chemical structure of the polyelectrolytes and lubricants  |
| S-3   | Abrasion durability of the SLIC film   |
| S-4   | Transmittance spectra of the SLIPS and SLIC films  |
| S-5   | Movies of hot water test   |
| S-6-9 | Water contact angle and sliding angle of the SLIC film prepared under various conditions                   |
| S-10  | Absorbance spectra of SLIC film and LbL film with silver ions  |
| S-11  | Water contact angles and sliding angles of the SLIC film before and after chemical and physical treatments |
| S-12  | Schematic of SLIC film works presumed to slide high and low surface-tension liquids                        |

## Chemical structure of the polyelectrolytes and lubricants

Poly(acrylic acid) (PAA, MW = 250,000, 35% aqueous solution, Aldrich), poly(allylamine hydrochloride) (PAH, MW = 120,000–200,000, Polysciences), PMHS (KF-99, viscosity: 20 mm<sup>2</sup>/s at 25 °C, Shin-Etsu Chemical), polydimethylsiloxane (PDMS, KF-96-30cs, viscosity: 30 mm<sup>2</sup>/s at 25 °C, Shin-Etsu Chemical), and amine-modified polydimethylsiloxane (APDMS, KF-868, viscosity: 90 mm<sup>2</sup>/s at 25 °C, Shin-Etsu Chemical) were used as polyelectrolytes and lubricants, respectively. The chemical structure of the polyelectrolytes and lubricants are shown in Figure S1.

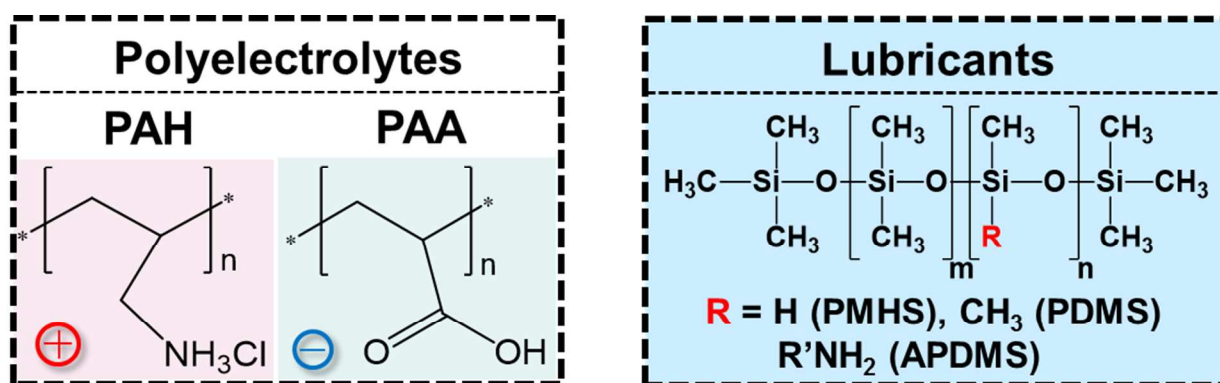


**Figure S1.** Chemical structure of the polyelectrolytes and lubricants used in this study.

### Abrasion durability of the SLIC film

The contact angle of the SLIC film almost had no change and the sliding angle was still below  $40^\circ$  after 10 cycles of abrasion against cotton soaked with ethanol (Figure S2). The durability of the SLIC film was higher than that of the SLIPS.

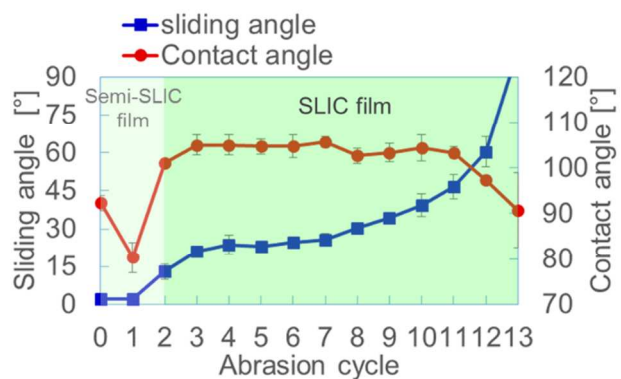


**Figure S2.** Contact angle and sliding angle change of SLIC film with cycle of abrasion against cotton soaked with ethanol.

### Transmittance spectra of SLIPS and SLIC films

The transparency of the SLIC film was compared with that of the SLIPS (Figure S3). The transparencies of the two samples were similar, and the transmittance of SLIC film is more than 85 % in a visual light range.

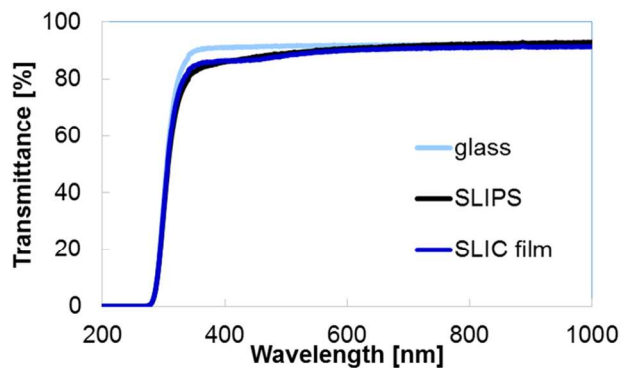


**Figure S3.** UV–visible absorption spectrometer (UV-vis) transmittance spectra of SLIPS and the SLIC film and slide glass used as substrate.

### **Movies of hot water test**

- Supporting Information Movie S1 (.mp4, 18.0M byte)
- Supporting Information Movie S2 (.mp4, 15.1M byte)

We performed a hot water test to further examine the properties of these samples (see Movies S1 and S2). The hot water test involved the following steps: first, several droplets (10 mL) of hot distilled water were put on the surface of the SLIPS and the semi-SLIC film, which were tilted at an angle of 40°; second, the films were washed with acetone and dried under an air flow; and finally, several droplets of hot water were put on the surface of these films. Movie S2 shows the results of thermography measurements during the hot water test, which confirmed the use of heated water (60–70 °C) and the evaporation of acetone. However, the SLIPS became cloudy after washing, and the hot water droplets remained pinned on its surface because the rough underlayer was exposed. In contrast, the SLIC film displayed behavior similar to that of the semi-SLIC film, clearly indicating that the SLIC film maintained its slipperiness.

## **Water contact angle and sliding angle of the SLIC film prepared under various conditions**

We examined the performance of SLIC films prepared under various conditions for LbL formation and lubricant reaction with PMHS as the lubricant (Table S1). Sliding angle measurements showed that the optimal number of bilayers for the polyelectrolyte film was 7–8. When the number of bilayers was too small, the lubricant was only weakly immobilized owing to the low thickness of the polyelectrolyte film. On the other hand, it was difficult for water droplets to slide on a film with more than nine bilayers because such films have rough surfaces, as can be seen from the ellipsometry measurements, FE-SEM images, and laser microscope images (Figures S4, S5, and S6). In addition, the transmittance of the SLIC films decreased as the concentration of the silver acetate solution increased (Figure S7). The transparency of the SLIC film decreased after heat-treatment at 100 °C for 1 h to accelerate the reaction. This result indicates that the decrease in transparency was caused by the surface plasmon absorption of Ag nanoparticles formed through the oxidation–reduction reaction between Si–H groups and silver ions, as described in detail below. The increased sliding angle of the SLIC film prepared on the LbL film immersed in a 6 mM silver acetate solution might be attributable to the formation of a large number of Ag nanoparticles on the film surface and a decrease in the mobility of the lubricant owing to reaction with too many silver ions in the film. Moreover, the SLIC film exhibited a high degree of slipperiness after heat treatment at temperatures higher than 80 °C. The rate of the oxidation–reduction reaction decreases with decreasing temperature.

**Table S1.** Water contact angle and sliding angle of the SLIC film prepared under various conditions.

| Bilayers    | Silver acetate concentration | Reaction temperature | Reaction time | Contact angle [°] |            | Sliding angle [°] |            |
|-------------|------------------------------|----------------------|---------------|-------------------|------------|-------------------|------------|
|             |                              |                      |               | Ave.              | S.D.       | Ave.              | S.D.       |
| 3 bi        | 2 mM                         | 100 °C               | 1 Hr          | 101               | 0.8        | 47                | 2.4        |
| 6 bi        | 2 mM                         | 100 °C               | 1 Hr          | 105               | 1.2        | 36                | 7.6        |
| <b>7 bi</b> | <b>2 mM</b>                  | <b>100 °C</b>        | <b>1 Hr</b>   | <b>105</b>        | <b>0.0</b> | <b>31</b>         | <b>5.6</b> |
| 8 bi        | 2 mM                         | 100 °C               | 1 Hr          | 104               | 4.1        | 30                | 2.1        |
| 9 bi        | 2 mM                         | 100 °C               | 1 Hr          | 105               | 2.4        | 36                | 3.3        |
| 15 bi       | 2 mM                         | 100 °C               | 1 Hr          | 109               | 0.9        | 56                | 26.6       |
| 7 bi        | 1 mM                         | 100 °C               | 1 Hr          | 105               | 1.2        | 32                | 1.6        |
| <b>7 bi</b> | <b>2 mM</b>                  | <b>100 °C</b>        | <b>1 Hr</b>   | <b>105</b>        | <b>0.0</b> | <b>31</b>         | <b>5.6</b> |
| 7 bi        | 4 mM                         | 100 °C               | 1 Hr          | 102               | 0.5        | 28                | 1.7        |
| 7 bi        | 6 mM                         | 100 °C               | 1 Hr          | 92                | 1.2        | >90               | -          |
| 7 bi        | 2 mM                         | 60 °C                | 1 Hr          | 98                | 1.9        | >90               | -          |
| 7 bi        | 2 mM                         | 60 °C                | 3 Hr          | 101               | 1.9        | 77                | 12.5       |
| 7 bi        | 2 mM                         | 80 °C                | 1 Hr          | 103               | 0.0        | 33                | 3.9        |
| <b>7 bi</b> | <b>2 mM</b>                  | <b>100 °C</b>        | <b>1 Hr</b>   | <b>105</b>        | <b>0.0</b> | <b>31</b>         | <b>5.6</b> |
| 7 bi        | 2 mM                         | 120 °C               | 1 Hr          | 105               | 0.8        | 32                | 2.1        |
| 7 bi        | 2 mM                         | 150 °C               | 1 Hr          | 103               | 0.8        | 29                | 5.0        |

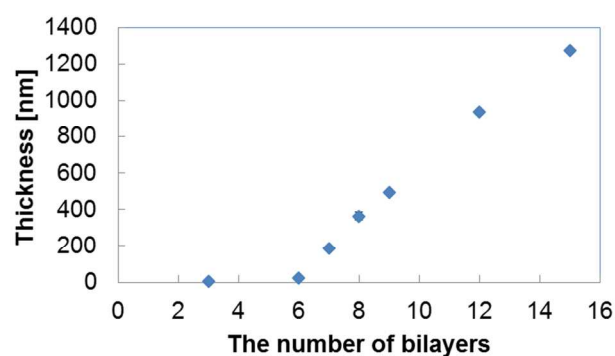


**Figure S4.** Relationship between film thickness and bilayers of the LbL films.

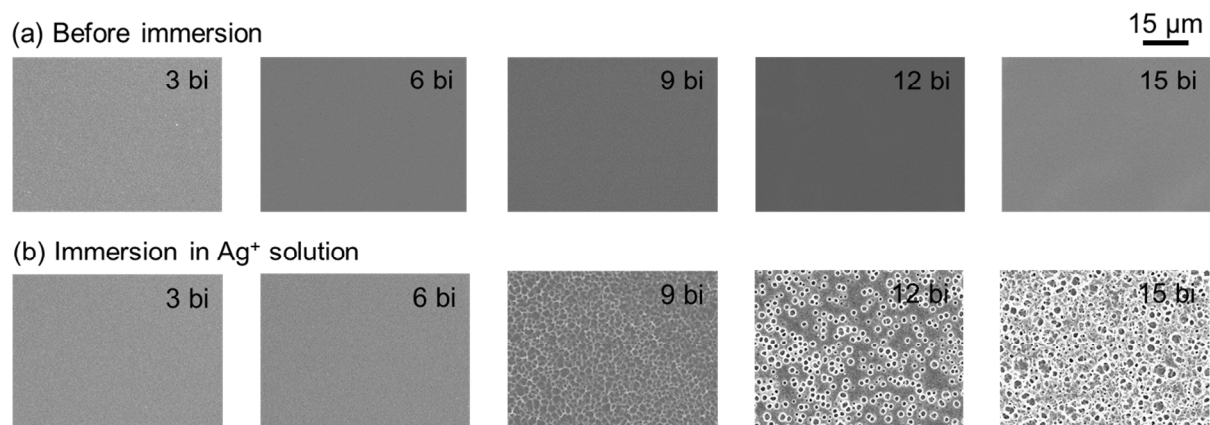


**Figure S5.** Field emission scanning electron microscopy (FE-SEM) surface images of the LbL films (bilayers = 3, 6, 9, 12, 15) before and after immersion in 1 mM silver acetate aqueous solution.

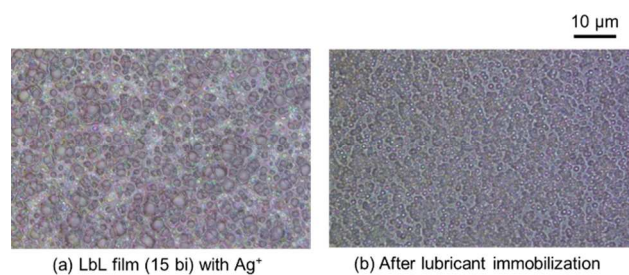


**Figure S6.** Laser microscope images of the LbL films (15 bilayers) with silver ions before and after lubricant immobilization.

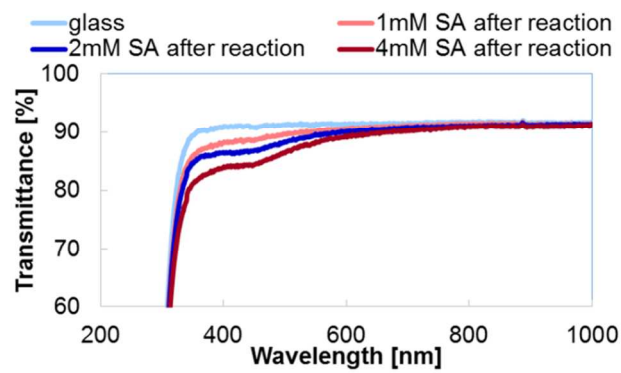


**Figure S7.** UV-vis transmittance spectra of the SLIC films as a function of silver acetate solution concentration and slide glass used as substrate.

### Absorbance spectra of SLIC film and LbL film with silver ions

Only the UV-vis absorbance spectrum of the SLIC film showed an absorption peak, which was centered at approximately 440 nm (Figure 3b). Figure S8 shows the absorbance spectra of the SLIC film and the LbL film with silver ions as functions of the concentration of the silver acetate solution. The LbL film exhibited absorbance only after it reacted with PMHS, with the absorbance increasing with the amount of silver ions incorporated. These results indicate that the observed absorbance is related to surface plasmon absorption of Ag nanoparticles formed by the reduction of Ag ions to Ag metal. The particle size of the Ag nanoparticles (60–80 nm) was estimated from the absorption peak.

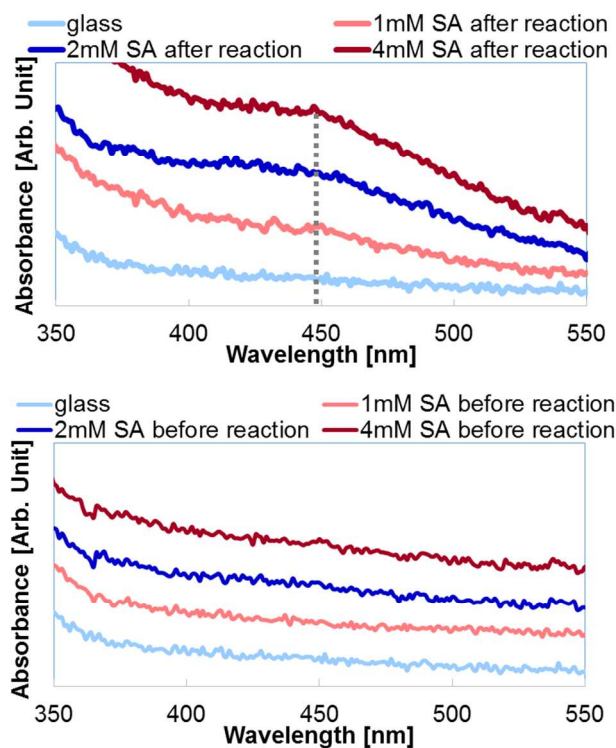


**Figure S8.** UV-vis absorption spectrometer absorbance spectra of SLIC film and LbL film as a function of silver acetate solution concentration and slide glass used as substrate.

## Water contact angles and sliding angles of the SLIC film before and after chemical and physical treatments

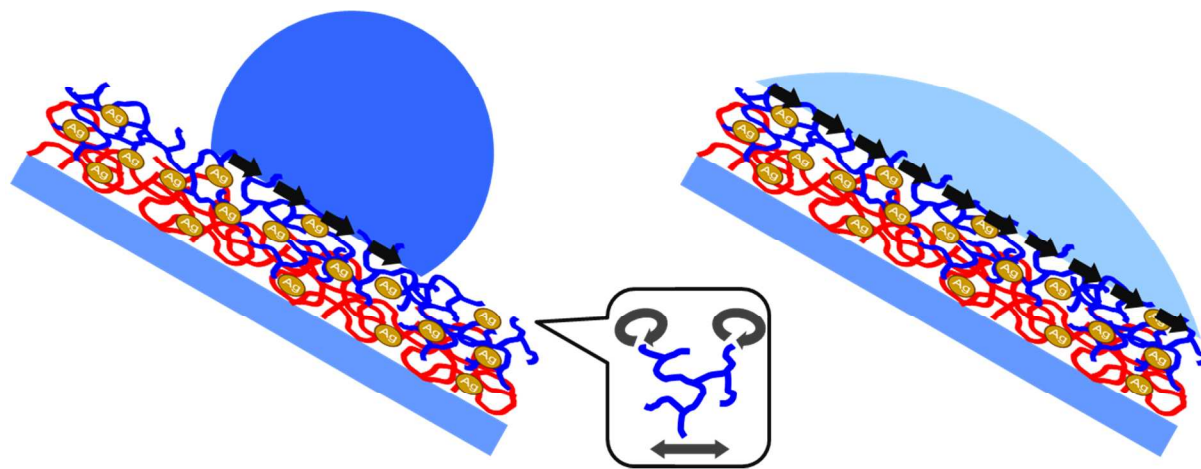
The water repellence and slipperiness of the SLIC film before and after chemical and physical treatments in a similar way of the SLIPS is shown in Table S2. The SLIC film also continued to exhibit slipperiness after chemical and physical treatments.

**Table S2.** Water contact angles and sliding angles of the SLIPS, semi-SLIC film, and SLIC film before and after chemical and physical treatments.

|  | Contact angle [°] |                |           | Sliding angle [°] |                |           |
|--|-------------------|----------------|-----------|-------------------|----------------|-----------|
|  | SLIPS             | Semi-SLIC film | SLIC film | SLIPS             | Semi-SLIC film | SLIC film |
| Before treatment                                       | 93                | 92             | 105       | 1                 | 2              | 31        |
| After spinning at 6000 rpm for 5 min                   | 105               | 96             | 105       | 6                 | 2              | 31        |
| After abrasion test against cotton soaked with ethanol | 92                | 80             | 103       | >90               | 4              | 34        |
| After immersion in acetone for 1 h                     | 121               | 102            | 102       | 84                | 27             | 38        |
| After ultrasonication in acetone for 1 min             | 138               | 104            | 104       | >90               | 32             | 34        |

### Schematic of SLIC film works presumed to slide high and low surface-tension liquids

The lubricant was immobilized on the LbL film as a poorly cross-linked gel with high mobility. In addition, PMHS itself has a highly mobile siloxane chain characterized by Si–O bonds with long interatomic distances and low barriers to rotation, which enhance the mobility of the lubricant gel. On tilting, the siloxane chains are moved by a force acting at a horizontal angle to the substrate, and thus liquid on the surface of the film also moves. Low-surface-tension liquids are moved by a weak force (low tilting angle) because many siloxane chains move the liquids owing to the large contact area (low contact angle) (Scheme S1). Therefore, the high degree of slipperiness might result from the mobility of the lubricant gel on the surface of the SLIC films, which is not a solid but rather a liquid-like material.



**Scheme S1.** Schematic of SLIC film works presumed to slide high and low surface-tension liquids.